

HIV-1 Tat and cocaine impact astrocytic energy reservoirs and epigenetic regulation by influencing the LINC01133-hsa-miR-4726-5p-NDUFA9 axis

Mayur Doke,¹ Jay P. McLaughlin,² James J. Cai,³ Gurudutt Pendyala,⁴ Fatah Kashanchi,⁵ Mansoor A. Khan,¹ and Thangavel Samikkannu¹

¹Department of Pharmaceutical Sciences, Irma Lerma Rangel College of Pharmacy, Texas A&M University, TX 78363, USA; ²Department of Pharmacodynamics, College of Pharmacy, University of Florida, Gainesville, FL 32611, USA; ³Veterinary Integrative Biosciences, Texas A&M University, TAMU 4458, College Station, TX 77845, USA; ⁴Department of Anesthesiology, University of Nebraska Medical Center (UNMC), Omaha, NE 68198, USA; ⁵National Center for Biodefense and Infectious Disease, Laboratory of Molecular Virology, George Mason University, Manassas, VA 20110, USA

Clinical research has proven that HIV-positive (HIV⁺) individuals with cocaine abuse show behavioral and neurocognitive disorders. Noncoding RNAs (ncRNAs), such as long ncRNAs (lncRNAs) and microRNAs (miRNAs), are known to regulate gene expression in the contexts of HIV infection and drug abuse. However, there are no specific lncRNA or miRNA biomarkers associated with HIV-1 Transactivator of transcription protein (Tat) and cocaine coexposure. In the central nervous system (CNS), astrocytes are the primary regulators of energy metabolism, and impairment of the astrocytic energy supply can trigger neurodegeneration. The aim of this study was to uncover the roles of lncRNAs and miRNAs in the regulation of messenger RNA (mRNA) targets affected by HIV infection and cocaine abuse. Integrative bioinformatics analysis revealed altered expression of 10 lncRNAs, 10 miRNAs, and 4 mRNA/gene targets in human primary astrocytes treated with cocaine and HIV-1 Tat. We assessed the alterations in the expression of two miRNAs, hsa-miR-2355 and hsa-miR-4726-5p; four lncRNAs, LINC01133, H19, HHIP-AS1, and NOP14-AS1; and four genes, NDUFA9, KYNU, HKDC1, and LIPG. The results revealed interactions in the LINC01133-hsa-miR-4726-5p-NDUFA9 axis that may eventually help us understand cocaine- and HIV-1 Tat-induced astrocyte dysfunction that may ultimately result in neurodegeneration.

INTRODUCTION

HIV-associated neurocognitive disorders (HANDs) include cognitive, behavioral, and mood disorders in HIV-infected patients, and 30%–50% of HIV-positive individuals manifest these symptoms.^{1,2} Although antiretroviral therapy (ART) has become more advanced and is currently available, there is no definitive cure to manage symptoms such as memory loss, impaired judgment, psychosis, and poor coordination of motor movements in HIV-positive individuals.³ Cocaine is one of the most common psychostimulant drugs of abuse among HIV patients and has been shown to

contribute to the progression of the infection to AIDS.⁴ Moreover, cocaine is known to accelerate neuroinflammation and HAND symptoms.^{5,6} ART is a necessary treatment to suppress viral load and maintain CD4 levels in the blood. Antidepressants and antipsychotic drugs can help relieve some HAND symptoms, but there is no prompt treatment or cure for HAND progression.^{1,2} Astrocytes are the primary energy reservoirs in the brain and maintain cellular functions, including energy fuel transfer and oxidative metabolism.^{7,8} Previous studies have shown that HIV infection and the HIV-Transactivator of transcription protein (Tat) and gp120 proteins can impact astrocyte networks and may be involved in HANDs.^{7,8} In addition, there is a strong correlation between astrocyte cell death mechanisms and neurological disease progression in HANDs,⁹ which can impair several cellular functions, including by causing epigenetic changes in the expression of messenger RNAs (mRNAs) and microRNAs (miRNAs).⁹ Previous research reports have shown that Transactivator of transcription protein (Tat) significantly alters protein-coding and noncoding regions of DNA in the contexts of HIV infection and cocaine exposure.^{10–15} Interestingly, both miRNAs, which are small (18- to 25-nt) single-stranded RNAs, and long noncoding RNAs (lncRNAs), which have more than 200 nt, are noncoding RNAs (ncRNAs) that can exert regulatory functions at different levels of gene expression, including at the chromatin-modification and posttranscriptional levels.¹⁶ miRNAs and lncRNAs interact with mRNAs, proteins, and DNA by acting as signals, decoys, scaffolds, and guides in various diseases.^{16–19} Previous research has shown that lncRNAs and miRNAs regulate gene expression in HIV infection and drug abuse.^{14,15,20} However, no specific lncRNA and miRNA biomarkers are associated with neuronal impairments caused by HIV-1 Tat and cocaine

Received 15 February 2022; accepted 4 July 2022;
<https://doi.org/10.1016/j.omtn.2022.07.001>

Correspondence: Thangavel Samikkannu, PhD, Department of Pharmaceutical Sciences, Irma Lerma Rangel College of Pharmacy, Texas A&M University, 1010 W Avenue B, Kingsville, TX 78363, USA.

E-mail: thangavel@tamu.edu



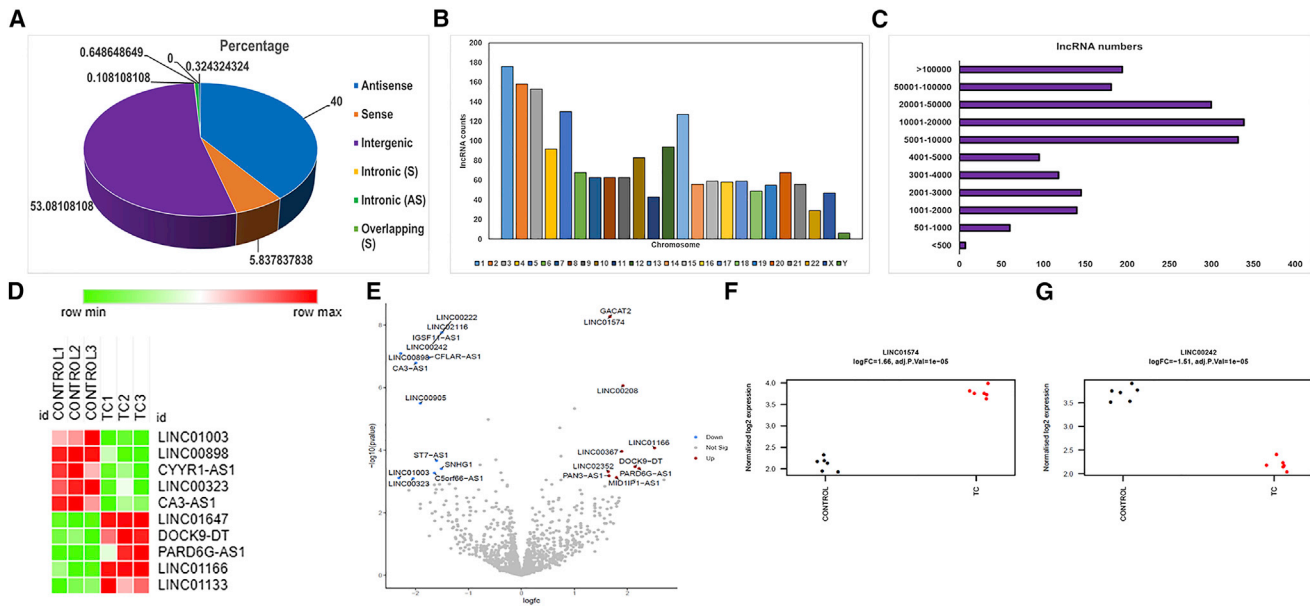


Figure 1. Summary of lncRNAs in TC-exposed human primary astrocytes compared with control astrocytes

(A) lncRNA subclass distribution given in percentages. (B) Chromosome location. (C) Size ranges and abundance. (D) Heatmap showing the top upregulated lncRNAs (colored red) and downregulated lncRNAs (colored green). (E) Volcano plot presenting the differential expression of lncRNAs. The x axis corresponds to FCs of -2 (downregulation) and $+2$ (upregulation). The y axis represents the $-\log_{10}$ p value. The red and green points in the plot represent the significant DE lncRNAs. The table shows the top upregulated and downregulated lncRNAs with the \log_2 FC values. (F and G) Stripcharts showing the significantly expressed lncRNAs with their individual expression values in each sample. The expression of LINC01674 was upregulated and that of LINC0242 was downregulated in the TC group compared with the control group ($p < 0.05$).

coexposure. Moreover, studies have shown that mRNAs/genes can be regulated through mechanisms independent of lncRNA-miRNA interactions.²¹ Therefore, abnormal expression of lncRNAs and miRNAs may dysregulate downstream target gene signaling, leading to alterations in cellular, biological, and molecular processes.²²

Therefore, we analyzed the effects of HIV-1 Tat and cocaine exposure on miRNA and lncRNA expression profiles in human primary astrocytes by utilizing small-RNA and whole-RNA sequencing (RNA-seq) analyses. Bioinformatics analysis revealed that HIV-1 Tat and cocaine coexposure significantly altered lncRNAs and miRNAs. We identified a specific list of significantly altered miRNAs and lncRNAs through systematic integrative bioinformatics and cellular/molecular experimental analyses. The gene/mRNA targets of the key identified miRNAs and lncRNAs were deciphered based on databases such as LncExpDB, miRWalk2.0, and miRNet. The target gene list showed the featured seven genes that were involved in brain energy metabolism and neurodegeneration pathways. Out of the seven genes, we selected four for both *in vitro* and *in vivo* studies to decipher the effect of coexposure to HIV-1 Tat and cocaine: NADH:ubiquinone oxidoreductase subunit A9 (NDUFA9); lipase G, endothelial type (LIPG); kynureninase (KYNU); and hexokinase domain-containing 1 (HKDC1). The systemic analysis results ultimately identified two significantly altered miRNAs, hsa-miR-2355 and hsa-miR-4726-5p; four lncRNAs, LINC01133, H19, HHIP-AS1, and NOP14-AS1; and two genes,

NDUFA9 and LIPG. Interestingly, lncRNA-miRNA-mRNA axis regulation was confirmed by knocking down the expression of LINC01133 in astrocytes. The small interfering RNA (siRNA)-mediated knockdown of LINC01133 resulted in downregulation of NDUFA9 and upregulation of hsa-miR-4726-5p. This integrated analysis reveals the alterations in lncRNA-miRNA-mRNA expression in cocaine- and HIV-1 Tat-treated human primary astrocytes. The results regarding the interactions in the LINC01133-hsa-miR-4726-5p-NDUFA9 axis may aid in understanding of cocaine- and HIV-1 Tat-induced astrocyte dysfunction and associated neurodegeneration.

RESULTS

Analysis of lncRNAs expression in HIV-1 Tat- and cocaine-exposed human primary astrocytes

The whole-RNA-seq analysis results revealed that HIV-1 Tat, cocaine, and coexposure of HIV-1 Tat with cocaine significantly altered expression of lncRNAs. Research studies have shown that lncRNAs mainly interact and exert their action on nearby protein-coding gene targets.²³ We classified lncRNAs on the basis of their genomic locations. Based on this classification, significantly differentially expressed (DE) lncRNAs in the coexposure of HIV-1 Tat with cocaine group were found to be 53.08% intergenic, 40% antisense, and 5.83% (321) sense (Figure 1A) in the genome. lncRNAs were distributed in all chromosomes, and the highest number of lncRNAs

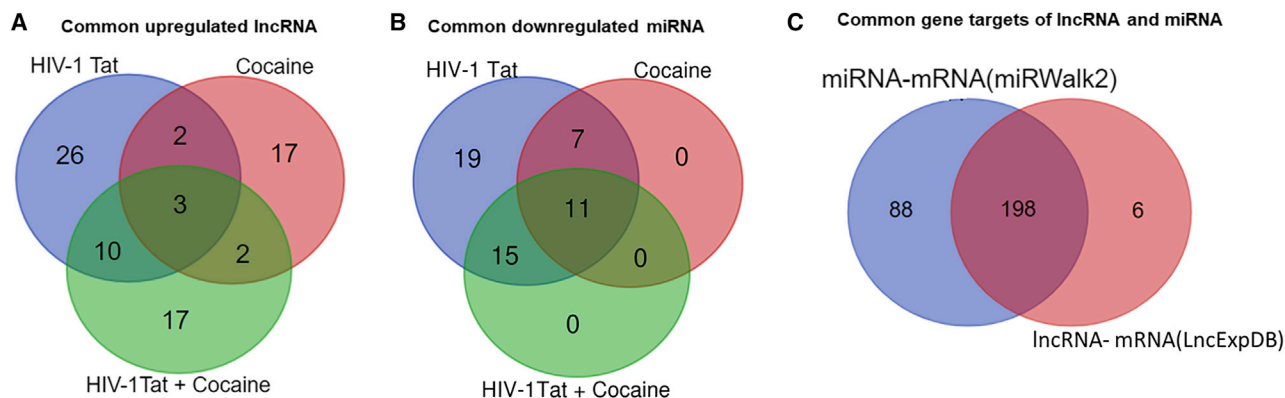


Figure 2. Identification of significant lncRNAs, miRNAs, and lncRNA/miRNA-targeted mRNAs

(A) Venn diagram showing the upregulated DE lncRNAs in the different group comparisons. Three lncRNAs—LINC01133, LINC01016, and LINC02352—were shared among all three comparisons (control versus HIV-1 Tat, control versus cocaine, and control versus TC). (B) Venn diagram showing the downregulated DE miRNAs among the different group comparisons. Eleven miRNAs—miR6799, miR6756, miR4734, miR4483, miR551A, miR6743, miR2355, miR4726, miR4786, miR597, and miR5580—were shared among all three comparisons. (C) The miRNA-specific gene targets were determined with the help of the miRWalk 2.0 web server, and the lncRNA-targeted mRNAs were identified using LncExpDB. The Venn diagram shows the 198 commonly identified gene targets among the miRNA-mRNA and lncRNA-mRNA comparison groups.

belonged to chromosome 1 (Figure 1B). These lncRNAs ranged from 100 to 709,352 nt in size (Figure 1C).

Identification of DE lncRNAs

To decode the effects of cocaine and HIV-1 Tat exposure on lncRNAs in human primary astrocytes, we investigated the DE lncRNAs between the control and HIV-1 Tat- and cocaine-exposed samples. Our study's primary goal was to determine whether cocaine and HIV-1 Tat exposure dysregulate lncRNA expression, which may affect gene expression posttranscriptionally. To explore the lncRNA-level changes, we used thresholds of a fold change (FC) ≥ 1.5 and $p \leq 0.05$. First, we explored lncRNA expression in HIV-1 Tat-exposed samples compared with control samples. The read counts from control and HIV-1 Tat-exposed samples were transformed to \log_2 (counts per million [CPMs]) values. The normalization of the data was performed using a mean-variance relationship model with precision weights in the voom method. A total of 54 lncRNAs were significantly altered, and out of the 48, 6 lncRNAs were downregulated, while 42 lncRNAs were upregulated (Data S1). The heatmap shows the most significantly upregulated and downregulated lncRNAs (Figure S1A). Figure S1B shows a volcano plot showing the upregulated and downregulated lncRNAs with \log_2 FC values and significant p values. Moreover, the lncRNA expression values in control and HIV-1 Tat-exposed samples were compared by plotting the normalized \log_2 FC expression levels for LINC01133 and LINC00222 (Figures S1C and S1D). Next, we evaluated the DE analysis between control and cocaine-exposed human primary astrocytes. Cocaine exposure to astrocytes significantly altered 37 lncRNAs compared with control. Of the 37 lncRNAs, 26 lncRNAs and 11 lncRNAs were significantly upregulated and downregulated, respectively. Figure S2A shows the upregulated and downregulated lncRNA expression in the form of a heatmap. The volcano plots in Figure S2B depict the most significant upregu-

lated and downregulated lncRNAs. Moreover, the lncRNA expression values in the control and cocaine-exposed samples were compared by plotting the normalized \log_2 FC expression values for LINC01133 and LINC01933 (Figures S2C and S2D; Data S2). Furthermore, we evaluated the effect of combined exposure to HIV-1 Tat and cocaine (TC) on lncRNA expression in human primary astrocytes. The coexposure significantly changed lncRNA expression levels and mainly affected LINC01133, LINC00323, and LINC01166, as shown by the heatmap in Figure 1D. These results revealed that 50 lncRNAs were significantly altered because of TC exposure. Of these lncRNAs, 33 lncRNAs were upregulated, while 17 lncRNAs were downregulated. The normalized \log_2 FC values of the lncRNAs between control and TC-treated astrocytes showed significant differences between the groups, as shown in the volcano plot in Figure 1E. Moreover, the lncRNA expression values in control and TC-exposed samples were compared by plotting the normalized \log_2 FC values for LINC01574 and LINC00242 (Figures 1F and 1G) (Data S3). In summary, the lncRNA-seq data indicated that TC exposure significantly altered lncRNA expression and induced dysregulation of lncRNAs in human primary astrocytes.

Next, we selected only significantly upregulated lncRNAs from the control versus HIV-1 Tat, control versus cocaine, and control versus TC comparisons. Then, we compared all the lncRNAs from the different group analyses and observed three common lncRNAs, LINC01133, LINC01016, and LINC02352 (Data S4), as shown in Figure 2A. A detailed list of the comparisons of all lncRNAs is given in Figure S3.

Analysis of lncRNA- and miRNA-targeted genes

lncRNAs and miRNAs are ncRNAs that regulate mRNA expression. lncRNAs change the expression of protein-coding genes at the

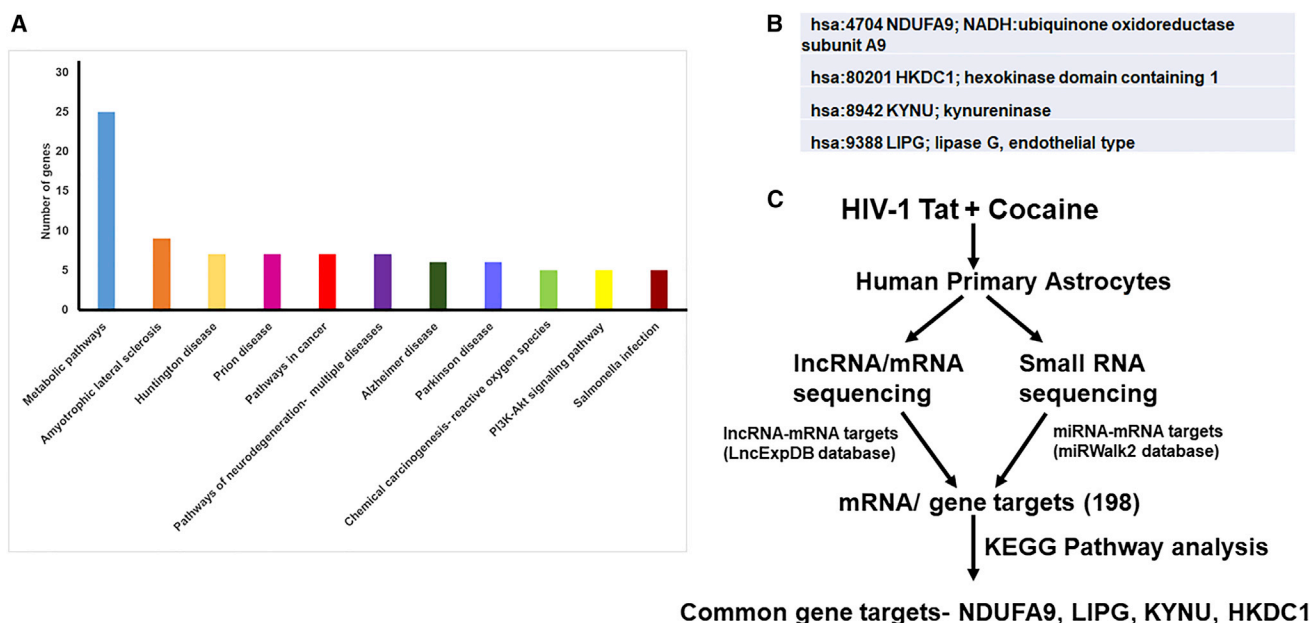


Figure 3. Functional analysis of miRNA- and lncRNA-targeted genes

(A) The involvement of the miRNA- and lncRNA-targeted genes in various pathways was investigated using KEGG pathway analysis. A list of the most enriched KEGG pathways in which the genes are involved is shown. (B) Genes associated with various components, metabolic pathways, and neurodegeneration pathways. The four common genes, NDUFA9, LIPG, KYNU, and HKDC1, are shown. (C) Gene target identification workflow. Schematic of the workflow used to analyze the miRNA-specific gene targets with the help of the miRWalk 2.0 web server. The lncRNA-targeted mRNAs were identified using LncExpDB.

posttranscriptional level by either serving as miRNA precursors or by regulating mRNAs via competition or interaction with miRNAs for target genes.²¹ In order to investigate the target genes of lncRNAs, we assessed the common gene targets of 17 lncRNAs from the comparisons by utilizing the LncExpDB database. The 17 lncRNAs were LINC01133, LINC01016, LINC02352, NOP14-AS1, LINC01164, CACNA1C-AS2, LINC01166, LINC00552, LINC00571, LINC02585, LINC02359, LINC02070, LINC00367, LINC02432, LY86-AS1, LINC00923, and GATA6-AS1, as shown in [Data S5](#). The LncExpDB database analysis revealed that these 17 lncRNAs targeted 204 mRNAs/genes. To identify the miRNA-targeted genes, we identified significantly downregulated miRNAs from the small-RNA-seq data ([Data S6](#)). We analyzed the small-RNA-seq data for all comparison groups such as control versus HIV-1 Tat, control versus cocaine, and control versus TC. We used the normalized miRNA expression value in each sample of the control and TC-exposed groups to create DE profiles across all the comparisons. A miRNA was considered DE when it had ≥ 10 reads in each sample, $FC \leq -1.5$, and $p \leq 0.05$. First, we explored miRNA expression in HIV-1 Tat-exposed samples compared with control samples. Our data analysis revealed that 11 common miRNAs were significantly downregulated across all comparisons ([Data S7](#)), as shown in [Figure 2B](#). These 11 miRNAs included miR6799, miR6756, miR4734, miR4483, miR551A, miR6743, miR2355, miR4726, miR4786, miR597, and miR5580. A detailed list of the miRNA comparisons is given in [Figure S4](#). We also evaluated miRNA-gene targets by utilizing the miRWalk 2.0 web server, which relies on databases such as TargetScan, miRDB, and miRTarBase.

We investigated the gene/mRNA targets of the 11 common downregulated miRNAs based on their binding capabilities in the 3' untranslated region (UTR), 5' UTR, and coding sequence (CDS). In total, 286 significant miRNA-targeted mRNAs/genes were arranged on the basis of their expression in all comparisons groups, such as control versus HIV-1 Tat, control versus cocaine, and control versus TC ([Data S8](#)). We mainly arranged genes from upregulation to downregulation and then selected only significantly upregulated genes for further analysis.

Furthermore, we compared the miRNA-targeted and lncRNA-targeted mRNA/gene lists and observed 198 common gene/mRNA targets, as shown in [Figure 2C](#). A detailed list of the miRNA- and lncRNA-targeted genes is given in [Figure S5](#).

Biological function and pathway analyses of the target genes of the common downregulated miRNAs and upregulated lncRNAs with the Kyoto Encyclopedia of Genes and Genomes (KEGG) and Gene Ontology (GO) databases

The 198 significant target mRNAs/genes of miRNAs and lncRNAs from the systematic bioinformatics analysis were identified based on their binding probability, number of pairings, and binding site positions within the seed regions. The GO annotation terms (from the GO Consortium) and the biological pathways (based on the curated KEGG pathways database) of the 198 target mRNAs/genes were explored, as shown in [Figure 3A](#). The results revealed that the genes were significantly associated with KEGG pathway terms, such as metabolic pathways, amyotrophic lateral sclerosis,

Huntington's disease, Parkinson's disease, Alzheimer's disease (AD), and pathway of neurodegeneration (Figure 3A). We also investigated the gene targets associated with various metabolic pathways (25 genes) and neurodegeneration pathways of multiple diseases (7 genes) (Data S9). Furthermore, we performed a Venn diagram analysis and observed four common genes representing both the metabolic pathways and the neurodegeneration pathways (Figure 3B): NDUFA9, LIPG, KYNU, and HKDC1. The schematic in Figure 3C explains the systematic approach for identification of these four gene targets. The KEGG pathway analysis of TC exposure gene targets indicate that gene targets mainly involve dysregulation of energy metabolism. This confirms our earlier findings that HIV-1 Tat and cocaine may impact astrocyte energy deficits and induce neurodegeneration.¹⁵

HIV-1 Tat and cocaine impact lncRNA and miRNA target protein levels in human primary astrocytes and an HIV-1 Tat-inducible transgenic (iTat) mouse model

The integrative miRNA-mRNA and lncRNA-mRNAs target prediction analysis revealed that 198 genes were potential targets of lncRNAs and miRNAs. We analyzed the involvement of these 198 genes in various KEGG pathways and found that 25 genes were significantly involved in metabolic pathways, while 7 genes were involved in neurodegenerative disease pathways, as shown in Figure 3B. We more closely investigated four genes (NDUFA9, LIPG, KYNU, and HKDC1) that were common to both metabolic and neurodegenerative disease pathways. We investigated the effects of HIV-1 Tat and cocaine on the proteins and observed slight upregulation of KYNU protein levels in the HIV-1 Tat, cocaine, and TC groups compared with the control group (Figure 4A). In addition, cocaine (F(3, 6) = 32.90, $p = 0.0005$), HIV-1 Tat (F(3, 6) = 32.90, $p = 0.0007$), and TC (F(3, 6) = 32.90, $p = 0.0030$) significantly upregulated HKDC1 protein levels (Figures 4E and 4F). Compared with the control, TC treatment also significantly upregulated NDUFA9 (F(3, 6) = 8.268, $p = 0.0199$) (Figures 4C and 4D) and LIPG (F(3, 6) = 9.562, $p = 0.0179$) protein levels (Figures 4G and 4H). We also investigated the effects of HIV-1 Tat and cocaine exposure on the mRNA expression of NDUFA9 and LIPG. Cocaine (F(3, 6) = 107.8, $p < 0.0001$), HIV-1 Tat (F(3, 6) = 107.8, $p = 0.0006$), and TC (F(3, 6) = 107.8, $p = 0.0013$) significantly upregulated NDUFA9 mRNA levels (Figure 4I), while cocaine (F(3, 6) = 18.4, $p = 0.0017$), HIV-1 Tat (F(3, 6) = 18.4, $p = 0.0057$), and TC (F(3, 6) = 18.4, $p = 0.0203$) significantly upregulated LIPG mRNA levels (Figure 4J).

We validated the effects of cocaine treatment in an HIV-1 iTat mouse model. We isolated brain tissues from HIV-iTat mice with and without 14 days of exposure to cocaine. We resolved the total protein extracts by sodium dodecyl sulfate-polyacrylamide gel electrophoresis (SDS-PAGE) and analyzed NDUFA9, LIPG, KYNU, and HKDC1 levels by western blotting. KYNU protein expression was significantly upregulated in the brain tissues of mice treated with HIV-1 Tat (F(3, 6) = 11.99, $p = 0.0071$), cocaine (F(3, 6) = 11.99, $p = 0.0167$), and TC (F(3, 6) = 11.99, $p = 0.0128$) compared with those of saline-treated mice (controls) (Figures 5A and 5B). We

also observed similar effects of HIV-1 Tat (F(3, 6) = 12.37, $p = 0.0092$) and cocaine (F(3, 6) = 12.37, $p = 0.0086$) on NDUFA9 (Figures 5C and 5D). HIV-1 Tat (F(3, 6) = 19.62, $p = 0.0025$), cocaine (F(3, 6) = 19.62, $p = 0.0025$), and TC (F(3, 6) = 19.62, $p = 0.0063$) significantly increased HKDC1 protein levels (Figures 5E and 5F). LIPG protein levels in HIV-1 iTat mice were significantly increased by cocaine (F(3, 6) = 7.535, $p = 0.0415$) and TC (F(3, 6) = 7.535, $p = 0.0183$) exposure (Figures 5G and 5H).

Identification of miRNA-lncRNA interactions

To identify miRNA-lncRNA interactions, we utilized the 33 significantly downregulated miRNAs from all comparison groups, such as control versus HIV-1 Tat, control versus cocaine, and control versus TC described previously (Data S6). We utilized the miRNet database, which consists of Cross-linking immunoprecipitation (CLIP) experiment-validated miRNA-targeted lncRNAs, to identify miRNA-lncRNA interactions. We observed 1,047 lncRNA-miRNA interactions (Data S10). A total of 18 of 33 miRNAs targeted lncRNAs. The resulting list of lncRNAs was parsed based on the significantly upregulated lncRNAs ($FC \geq 1.5$ and $p \leq 0.05$) observed in our RNA-seq data analysis. These significantly upregulated lncRNAs were then compared with the common lncRNAs we obtained from the analysis in Figure S3, as shown in Data S11. Furthermore, we investigated the association of lncRNAs with diseases by utilizing the LncBook disease database (Data S12). We compared the lncRNAs associated with neurodegenerative diseases with the lncRNAs in the curated list and obtained a list of 35 lncRNAs (Data S13). We assessed the target miRNAs of these 35 lncRNAs with the LncBase database, as shown in Figure S6. Of the 35 lncRNAs, only 17 showed miRNA interactions. A total of 1,046 lncRNA-miRNA interactions occurred in which 104 miRNAs were targeted by 17 lncRNAs (Data S14). However, only miR200c expression was downregulated in the small-RNA-seq data. We used the DIANA tools of LncBook to identify the most significant miRNA-lncRNA interactions for targeting of specific lncRNAs. To perform this detailed analysis, we utilized 11 common miRNAs from the list of significantly downregulated miRNAs across all comparison groups. We screened the interactions mainly between the 11 miRNAs and 35 lncRNAs based on validated CLIP experiments with the DIANA tools and found that 10 of the miRNAs (hsa-miR-1913, hsa-miR-2355, hsa-miR-4726, hsa-miR-873, hsa-miR-206, hsa-miR-5008, hsa-miR-6799, hsa-miR-4525, hsa-miR-4731, and hsa-miR-6823) showed significant interactions with 10 lncRNAs (TP53TG1, LBX2-AS1, LINC01197, LY86-AS1, LINC01133, LINC02432 (ENSG00000248810), HCP5, H19, HHIP-AS1, and NOP14-AS1) (Data S15). Of these 10 miRNAs, we selected 2 miRNAs that showed many interactions with the 10 lncRNAs, hsa-miR-2355 and hsa-miR-4726, for further investigation. These analyses identified potential miRNA-targeted lncRNAs that may play major roles as endogenous miRNA sponges.

Identification of potential interactions between lncRNAs and mRNAs

In order to decipher the possible interactions between lncRNAs and mRNAs, we utilized the LncRRISearch web server to predict specific mRNA targets of lncRNAs. The algorithm of LncRRISearch assesses

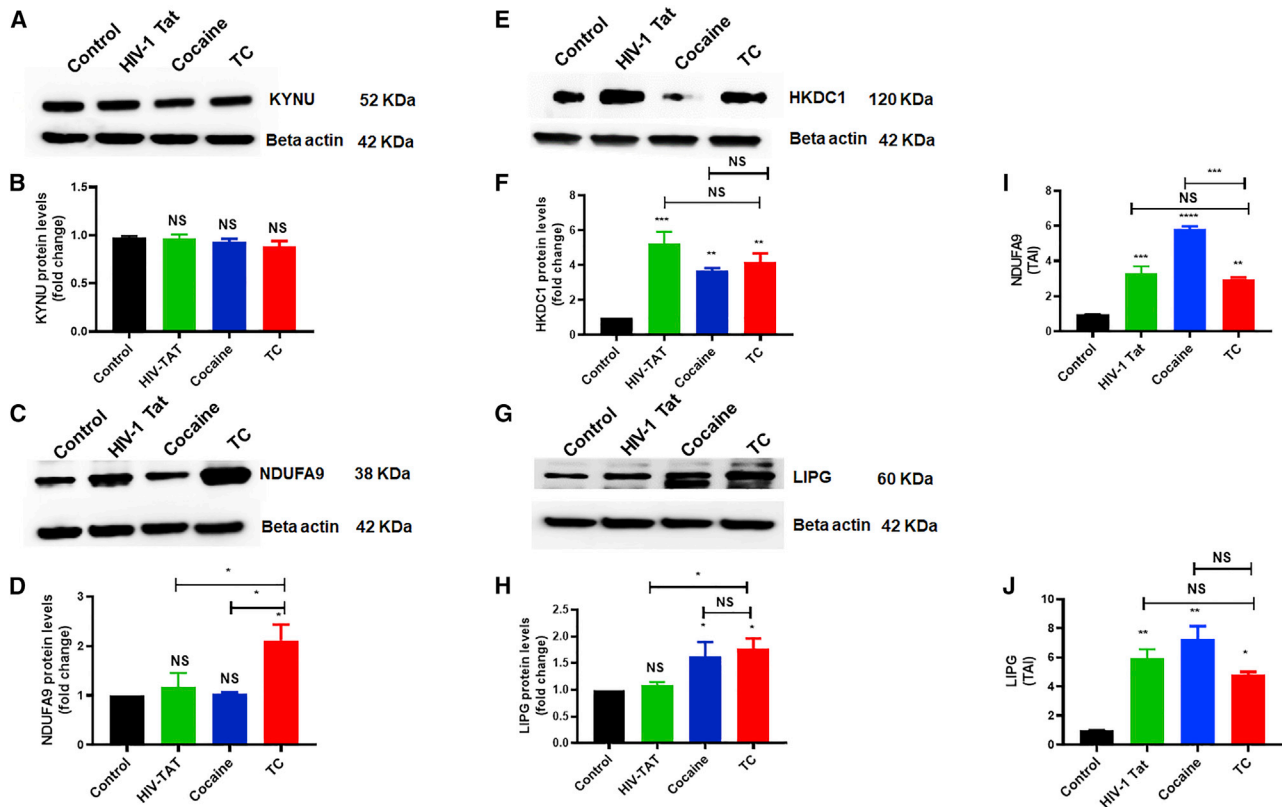


Figure 4. Effects of cocaine, HIV-1 Tat, and TC on miRNA- and lncRNA-targeted proteins in human primary astrocytes

Cells were exposed to cocaine (1 μ M) and HIV-1 Tat (50 ng/mL) either alone or in combination for 24 h. The protein expression levels of NDUFA9, LIPG, KYNU, and HKDC1 in astrocytes were determined by western blot analysis using β -actin as a loading control. The western blot shows (A) KYNU, (E) HKDC1, (C) NDUFA9, and (G) LIPG. The densitometric analysis results in (B), (D), (F), and (H) represent the protein levels (FC from control) of KYNU, HKDC1, NDUFA9, and LIPG, respectively. The data are expressed as the mean \pm SEM from three independent experiments. $n = 3$. Moreover, (I) NDUFA9 and (J) LIPG mRNA expression levels in astrocytes were determined by quantitative real-time PCR analysis using the housekeeping gene β -actin as a loading control. Two-way ANOVA was performed to compare the groups. The data are expressed as the mean \pm SEM of the transcript accumulation index (TAI) from three independent experiments. $n = 3$. **** $p < 0.0001$, *** $p < 0.001$, ** $p < 0.01$. NS, nonsignificant.

two RNA transcripts (the query lncRNA and the target RNA) for an arbitrary RNA-RNA interaction of interest. The threshold of the local base-pairing interaction energy calculated by RIBlast was set to -16 kcal/mol. The most stable local base-pairing interactions between the query and target RNAs are predicted by RIBlast. A lower interaction energy between two RNA transcripts indicates higher stability of the interaction. We assessed the interactions of the 10 lncRNAs (TP53TG1, LBX2-AS1, LINC01197, LY86-AS1, LINC01133, LINC02432 (ENSG00000248810), HCP5, H19, HHIP-AS1, and NOP14-AS1) and found that the miRNAs and lncRNAs targeted 29 genes/mRNAs, which were also assessed for their involvement in KEGG pathways (Data S16). The genes NDUFA9, LIPG, KYNU, and HKDC1 were targeted by more than seven lncRNAs. LINC01133, HHIP, H19, and NOPA-14 interacted with 7, 9, 24, and 12 gene/mRNA targets, respectively. Therefore, we investigated the expression of LINC01133, HHIP, H19, and NOPA-14 by polymerase chain reaction (PCR). Interestingly, RNA-seq data analysis revealed that LINC01133 was expressed significantly and upregulated in all comparison groups, such as control versus HIV-1 Tat, control

versus cocaine, and control versus TC. Moreover, we analyzed the interactions of LINC01133 with the gene targets NDUFA9, LIPG, KYNU, and HKDC1 and found that the LINC01133-NDUFA9, LINC01133-LIPG, and LINC01133-KYNU interactions had energies of -17.21 , -33.93 , and -59.80 kcal/mol, respectively, as shown in Figures 6A–6C. We identified lncRNA-miRNA interactions using the LncBook database and miRNA-lncRNA interactions using the miRNet database based on a systematic bioinformatics approach. The results revealed 4 gene targets, 10 miRNAs, and 10 lncRNAs. Further analysis with the LncRRISearch database demonstrated that LINC01133 is a potential target in the lncRNA-miRNA-mRNA axis. The schematic in Figure 6D explains the systematic approach used to investigate this axis.

HIV-1 Tat and cocaine impact lncRNA and miRNA expression in human primary astrocytes

We evaluated the effects of HIV-1 Tat and cocaine on the expression of lncRNAs that were selected through a careful systematic bioinformatics approach and with existing lncRNA databases, such as

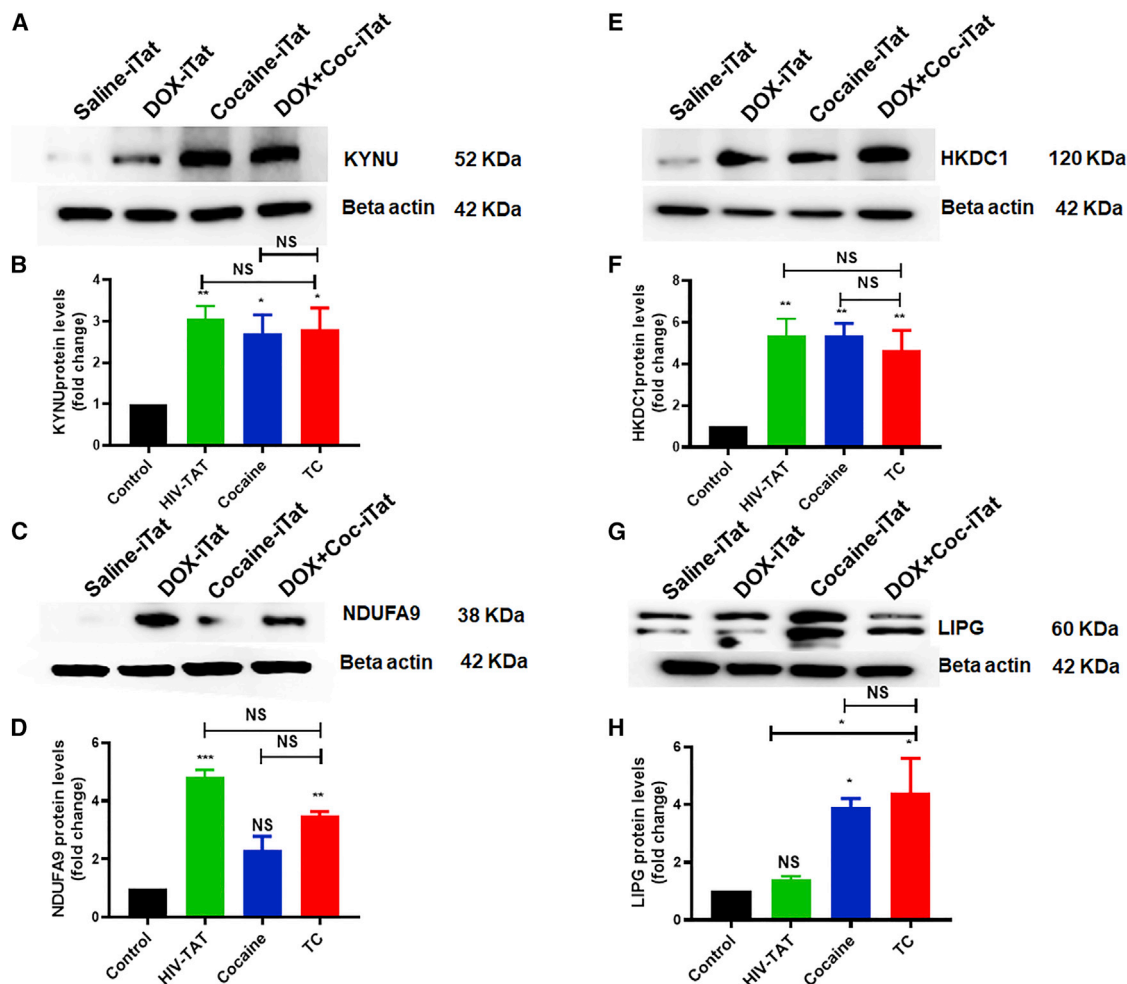


Figure 5. Effects of HIV-1 Tat, cocaine, and TC on the KYNu, HKDC1, NDUFA9, and LIPG proteins

HIV-1 iTat or saline-treated (control) mice received daily i.p. injections of saline or Dox (100 mg/kg/day) over 14 days with or without s.c. cocaine (10 mg/kg/day). Following treatment, equal amounts of protein lysates from harvested brains were resolved, and protein expression was analyzed using western blot analysis. The results show the levels of (A) KYNu, (E) HKDC1, (C) NDUFA9, and (G) LIPG in HIV-1 iTat (GT-tg) mouse brains and the levels of total β -actin protein. The densitometric analysis results in (B), (D), (F), and (H) represent the protein levels (FC from control) of KYNu, HKDC1, NDUFA9, and LIPG, respectively. The data are expressed as the mean \pm SEM from three independent experiments. The data represent three independent experiments. $n=3$, **** $p < 0.0001$, *** $p < 0.001$, ** $p < 0.01$, * $p < 0.05$.

LncExpDB, LncBase, and LncRRsearch. We investigated the significantly upregulated lncRNAs and performed PCR analysis on four of the lncRNAs: LINC01133, HHIP, H19, and NOPA-14. HIV-1 Tat (F(3, 6) = 23.34, $p = 0.0009$) and TC (F(3, 6) = 23.34, $p = 0.0044$) significantly upregulated LINC01133 expression (Figure 7A). H19 expression was significantly upregulated by exposure to HIV-1 Tat (F(3, 6) = 33.84, $p = 0.0025$), cocaine (F(3, 6) = 33.84, $p = 0.0108$), and TC (F(3, 6) = 33.84, $p = 0.0003$) (Figure 7B). Interestingly, HIV-1 Tat (F(3, 6) = 17.14, $p = 0.0030$), cocaine (F(3, 6) = 17.14, $p = 0.0072$), and TC (F(3, 6) = 17.14, $p = 0.0049$) also significantly upregulated NOPA-14 expression (Figure 7C). HHIP expression was also upregulated by HIV-1 Tat (F(3, 6) = 22.24, $p = 0.0055$), cocaine (F(3, 6) = 22.24, $p = 0.0062$), and TC (F(3, 6) = 22.24, $p = 0.0009$) (Figure 7D).

The expression of hsa-miR-2355 (F(3, 6) = 248.4, $p < 0.0001$) and hsa-miR-4726-5p (F(3, 6) = 47.72, $p < 0.0001$) was downregulated in astrocytes exposed to cocaine, HIV-1 Tat, and TC, as shown in Figures 7E and 7F, respectively.

Knockdown of LINC01133 in astrocytes downregulates NDUFA9 and upregulates hsa-miR-4726 expression

Previous studies have shown that lncRNAs and miRNAs can act as master regulators of various protein-coding genes.^{22,24} Moreover, lncRNAs can sequester miRNAs and inhibit interactions with their target mRNAs/genes.^{25,26} Bioinformatics analysis of the miRNet database showed that hsa-miR-4726-5p interacts with LINC01133. In addition, LncExpDB, LncBase, and LncRRsearch analyses demonstrated that the NDUFA9 protein-coding gene interacts

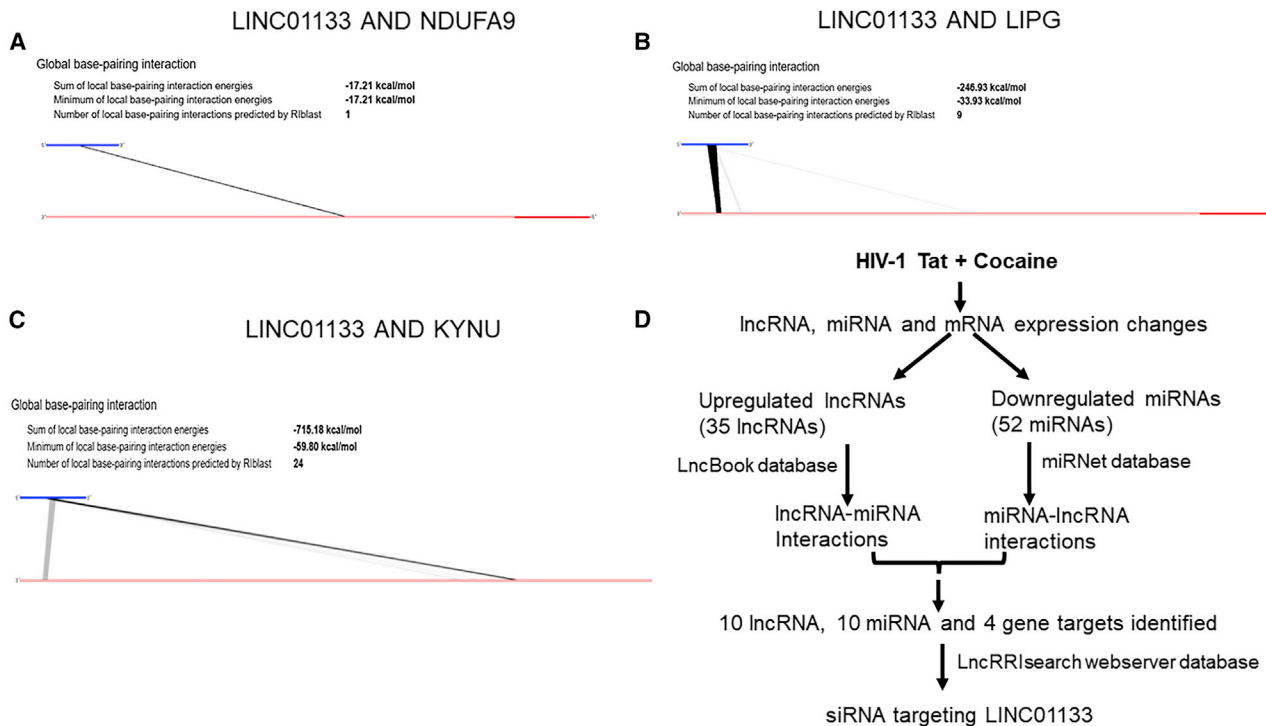


Figure 6. Identification of the interaction between lncRNAs and mRNA targets

The interactions between various lncRNAs and other lncRNAs or mRNAs were analyzed using LncRR|search. The interactions between LINC01133 and (A) NDUFA9, (B) LIPG, and (C) KYNU were analyzed and are illustrated with the minimum local pairing interaction energies. (D) Schematic of the workflow used to analyze the lncRNA-miRNA interactions with LncBook and the miRNA-lncRNA interactions with miRNet databases. The analysis identified 10 lncRNAs, 10 miRNAs, and 4 gene targets.

with LINC01133. Therefore, we next investigated whether LINC01133 could directly regulate NDUFA9 and hsa-miR-4726-5p in human primary astrocytes. To do this, we knocked down LINC01133 in human primary astrocytes by utilizing Silencer Select siRNA targeted to LINC01133. LINC01133 expression was significantly lower in the group transfected with siLINC01133 than in the negative control group (Figure 8A). LINC01133 expression was significantly downregulated by more than 80% in control and HIV-1 Tat-, cocaine-, and TC-treated human primary astrocytes (Figure 8A). We also compared NDUFA9 expression between siLINC01133-targeted astrocytes and negative control astrocytes (Figure 8B) and found that NDUFA9 expression was significantly downregulated in siLINC01133-targeted astrocytes in the control and HIV-1 Tat-, cocaine-, and TC-treated groups (Figure 8B). In order to confirm the gene-level changes revealed by quantitative real-time PCR, we also performed western blot analysis to assess the effects of HIV-1 Tat, cocaine, and TC on NDUFA9 protein expression. The results confirmed that NDUFA9 protein expression was significantly downregulated in siLINC01133-treated astrocytes compared with negative control astrocytes (Figure 8C). Furthermore, we examined the expression of hsa-mir-4726-5p in siLINC01133-treated astrocytes compared with negative control astrocytes. The results confirmed that hsa-mir-4726-5p expression was significantly upregulated in the control, HIV-1 Tat, cocaine,

and TC groups (Figure 8D), indicating that LINC01133 interacts with NDUFA9 and the hsa-miR-4726-5p network. The lncRNA-miRNA-mRNA network based on the bioinformatics and experimental results is shown in Figure 8E.

DISCUSSION

HIV infection and cocaine use are known to affect the transcription of mRNAs and the expression of lncRNAs and miRNAs.^{27,28} However, the orchestrated lncRNA-miRNA-mRNA molecular mechanism underlying the effects of HIV and cocaine use on dementia and neurocognitive behavior have not been reported. In this study, we investigated the molecular mechanism by which HIV-1 Tat and cocaine impact astrocyte energy metabolism to influence the lncRNA-miRNA-mRNA regulatory network, which may further induce neurodegeneration. This may in turn lead to dementia and neurocognitive and behavioral impairments. Dysregulated expression of miRNAs, mRNAs, and lncRNAs has been reported to play a critical role in the progression of neurodegeneration.^{29–31} Altered ncRNA expression has been identified as a pathogenesis marker in neuronal dysfunction-related diseases, such as AD and Parkinson's disease.^{32,33} Previous studies have demonstrated that lncRNAs can act as competitive endogenous RNAs (ceRNAs) that compete with target genes for miRNA response elements and attenuate the inhibitory effects of miRNAs on target genes.^{34,35} Therefore, lncRNAs can indirectly

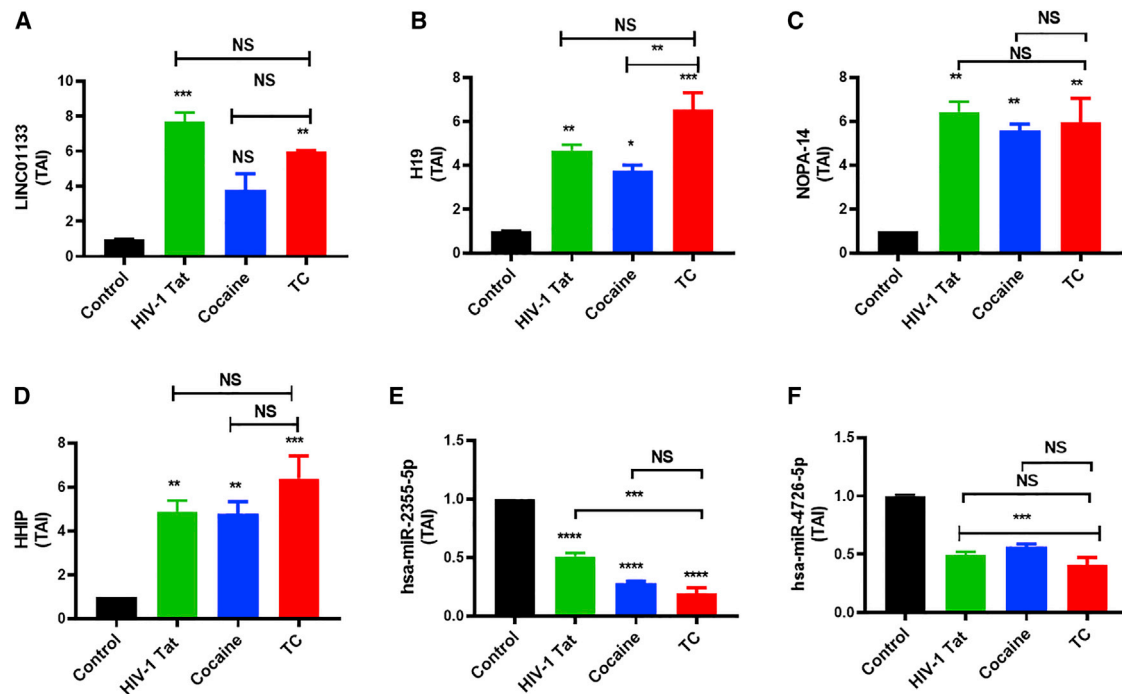


Figure 7. Effects of HIV-1 Tat, cocaine, and TC on miRNA and lncRNA expression

Human primary astrocytes were exposed to cocaine (1 μ M) and HIV-1 Tat (50 ng/mL) either alone or in combination for 24 h. Controls were maintained in drug-free medium (without drug exposure). (A) LINC01133, (B) H19, (C) NOPA-14, and (D) HHIP lncRNA expression levels in astrocytes were determined by quantitative real-time PCR analysis using the housekeeping gene β -actin as a loading control. Two-way ANOVA was performed to compare the groups. The data are expressed as the mean \pm SEM of the TAI from three independent experiments. $N = 3$. Moreover, (E) hsa-miR-2355-5p and (F) hsa-miR-4726-5p miRNA expression levels in astrocytes were determined by quantitative real-time PCR analysis using the housekeeping gene U6 snRNA as a loading control. The data are expressed as the mean \pm SEM of the TAI from three independent experiments. $n = 3$. **** $p < 0.0001$, *** $p < 0.001$, ** $p < 0.01$, * $p < 0.05$.

regulate the expression of target genes and affect the occurrence and development of diseases.³⁶

In addition to regulating transcription, lncRNAs control co-transcriptional regulatory functions and remodeling of chromatin structures.^{37–39} Thus, lncRNAs also notably contribute to perturbances in cellular metabolism. From the transcriptional perspective, miRNAs are considered negative gene regulators because they inhibit translation by degrading mRNA transcripts through association with the 3' UTRs of target gene sequences.⁴⁰ According to previous studies, the predominant downregulation of deregulated miRNAs in neurodegenerative diseases is attributed to upregulation of corresponding mRNAs and lncRNAs.^{20,41,42} Therefore, it is highly intriguing to explore the interplay of the lncRNA-miRNA-mRNA axis, which will provide the first insights into how these interactions influence downstream molecular processes.

In the present study, the integrative bioinformatics approach revealed that 10 miRNAs and 10 lncRNAs were significantly altered because of HIV-1 Tat and cocaine coexposure in the human primary astrocytes. The possible gene targets of these ncRNAs were identified based on bioinformatics and experimental evidence. We identified 198 gene targets, and their involvement in various biological processes was then analyzed with the KEGG database. KEGG analysis revealed seven common gene

targets that were heavily involved in neurodegeneration and metabolic pathways. Out of the seven, we selected four genes: NDUFA9, LIPG, KYNU, and HKDC1. Our *in vitro* and *in vivo* results showed that NDUFA9, LIPG, KYNU, and HKDC1 protein and mRNA expression levels were upregulated because of HIV-1 Tat and cocaine coexposure. A genome-wide association study analysis of an attention deficit hyperactivity disorder (ADHD) patient database has shown that HKDC1 is a significant highly expressed gene in ADHD patients.⁴³ The HKDC1 gene is positioned next to the hexokinase 1 (HK1) gene on chromosome 10^{44,45} and plays a significant role in glucose metabolism.⁴⁶ HKDC1 also plays an important role in regulating glycolytic activity, metabolic profiles, and glucose metabolism, which are mainly associated with energy metabolism.⁴⁷

Interestingly, our previously published and current research demonstrate that HIV infection, gp120, and Tat protein significantly activate HK1 gene activity in astrocytes and glia.^{48,49} Hexokinases phosphorylate glucose to produce glucose-6-phosphate (G6P), which is the most important and first step in most glucose metabolism pathways.⁵⁰ The HKDC1 and HK1 genes share 70% sequence homology at both the nucleotide and the amino acid levels.^{44,45} These findings suggest that HKDC1 may be involved in HIV-1 Tat- and cocaine-induced disruption of energy metabolism. In major depressive disorder (MDD) and

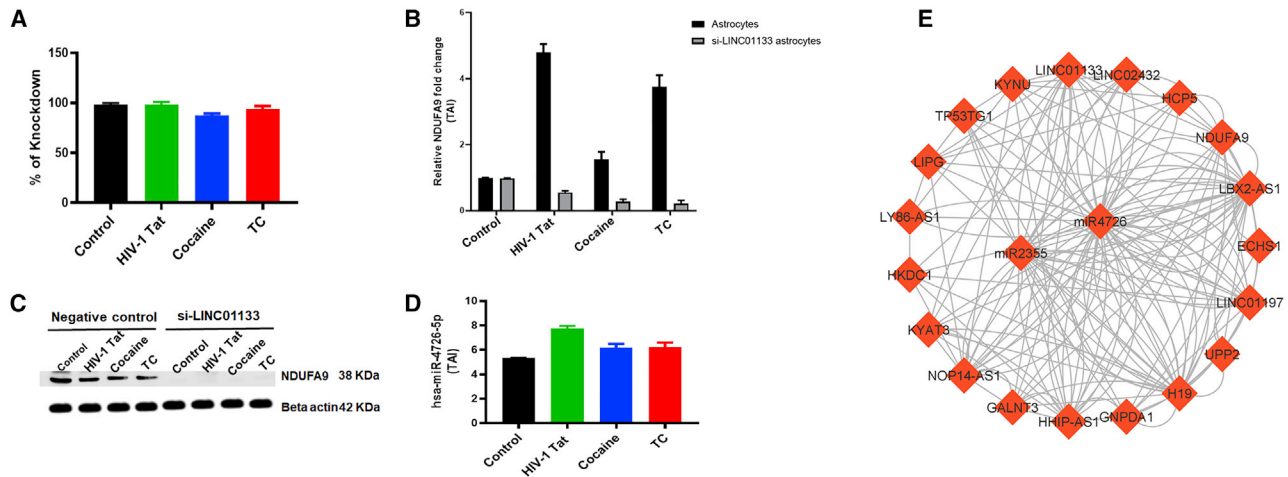


Figure 8. Effect of LINC01133 knockdown on cocaine- and HIV-1 Tat-treated human primary astrocytes

(A) Validation of the knockdown of the lncRNA LINC01133. Quantitative real-time PCR analysis demonstrated that the knockdown efficiency of LINC01133 was almost 90%. (B) Levels of NDUFA9 mRNA after knockdown of LINC01133 in HIV-1 Tat-, cocaine-, and TC-treated human primary astrocytes. (C) The protein expression levels of NDUFA9 in astrocytes were determined by western blot analysis using β -actin as a loading control. (D) hsa-miR-4726-5p miRNA expression was upregulated in astrocytes, as determined by quantitative real-time PCR analysis using the housekeeping gene U6 snRNA as a loading control. The data are expressed as the mean \pm SEM of the TAI from three independent experiments. $n = 3$. **** $p < 0.0001$, *** $p < 0.001$, ** $p < 0.01$, * $p < 0.05$. (E) LncRNA-miRNA-mRNA network. The rounded rectangles represent lncRNAs, the diamonds represent miRNAs, and the ellipses represent mRNAs. LncExpDB, LncBase, and LncRRIsearch database analyses revealed 10 lncRNA nodes, 2 miRNA nodes, and 8 mRNA nodes in the network.

bipolar disorder, the kynurenine (KYN) pathway (KP) plays a significant role in L-tryptophan (TRP) metabolism, producing several neurotoxic and neuroprotective metabolic precursors that may affect the astrocyte energy profile, possibly leading to neurodegeneration.⁵¹ HIV-1 Tat is known to activate indoleamine-2,3-dioxygenase (IDO), the rate-limiting enzyme of the KP, which further leads to increased TRP catabolism and generation of neurotoxins such as KYN.⁵² KYN has been shown to be a major player in the neuropathogenesis of HANDS.^{53,54}

HIV infection is known to limit the levels of TRP and successively increase the levels of the neurotoxin quinolinic acid in HIV-positive individuals, which leads to neuronal impairment with depression and cognitive impairment.⁵¹ The protein KYNU is involved in a KYN metabolic pathway leading to the production of nicotinamide adenine dinucleotide (NAD⁺).⁵⁵ It is well known that patients with cocaine use disorder (CUD) and comorbid conditions with MDD have significantly elevated levels of IDO/TRP 2,3-dioxygenase, KYN aminotransferase (KAT), and KYNU.⁵⁶

The protein NDUFA9 is a subunit of NADH:ubiquinone oxidoreductase (complex I of the electron transport chain [ETC]). NDUFA9 is a well-known regulator of the ETC and maintains mitochondrial respiratory complex I.⁵⁷ Dysregulation of NDUFA9 may impair ATP production and cause oxidative mitochondrial damage, which can further impact the mitochondrial genome.⁵⁸ Interestingly, an *in vivo* study recently showed that chronic cocaine self-administration in rats significantly alters the NDUFA9 protein and the network of proteins associated with NDUFA9.⁵⁹ LIPG and HK kinase play major roles in regulating metabolic profiles and oxidative energy resources to maintain

cellular homeostasis.⁶⁰ The enzyme LIPG plays vital roles in lipoprotein metabolism, cytokine expression, and lipid composition in cells. Previous studies have shown that LIPG expression alleviates inflammation and AD.⁶¹

HIV-1 Tat and cocaine use significantly influence miRNA-associated astrocyte energy metabolism,¹⁵ change mitochondrial DNA methylation,⁶² alter the expression of the energy sensor AMP-activated protein kinase,⁴⁹ cause redox modifications, and affect Nuclear Respiratory Factor (NRF) transcription.⁴⁸ These findings corroborate the results of the current study, which showed that lncRNAs and miRNAs target important common genes involved in neurodegeneration and metabolic pathways. We investigated the effects of HIV-1 Tat and cocaine coexposure on two miRNAs, hsa-miR-2355 and hsa-miR-4726-5p, that were selected with a systematic bioinformatics approach. The expression of both miRNAs was significantly downregulated. Moreover, we evaluated the expression of four lncRNAs, LINC01133, HHIP, H19, and NOPA-14, by PCR. The results revealed that these lncRNAs were significantly upregulated in HIV-1 Tat- and cocaine-coexposed human primary astrocytes. Intriguingly, LncExpDB, LncBase, and LncRRIsearch database analyses revealed that LINC01133 has increased degrees of interaction with NDUFA9 and hsa-miR-4726-5p. Fan et al. reported that the circular RNAs hsa_circ_0044520 and hsa_circ_0044529 play critical regulatory roles by sponging hsa-miR-4726-5p in laryngeal squamous cell carcinoma.⁶³ Interestingly, Ryu Hyun-Jung was granted a patent in 2019 for an invention related to a method for diagnosing neuronal degeneration in Parkinson's disease associated with miRNA biomarkers that can help prevent, ameliorate, or treat

Parkinson's disease. The miRNAs hsa-miR-494-3p, hsa-miR-1244, hsa-miR-6768-5p, and hsa-miR-4726-5p were significantly altered in a Parkinson's disease model and can be effectively used to diagnose and treat Parkinson's disease.⁶⁴ The data showed that hsa-miR-4726-5p was significantly downregulated from normal levels, which corroborates our findings in HIV-1 Tat- and cocaine-treated astrocytes. Previous studies have reported that LINC01133 is an oncogene in lung squamous cell carcinoma.⁶⁵ Recently, altered expression of LINC01133 was shown to be involved in the endothelial-to-mesenchymal transition process and various cancers, such as gastric cancer and lung and esophageal squamous cell carcinomas.^{66–69} In addition, HIV-1 Tat is known to recruit the zeste homolog 2 (EZH2) scaffold by inducing EZH2 phosphorylation in a reactive oxygen species (ROS)/Akt-dependent manner.⁷⁰ Intriguingly, ENCODE chromatin immunoprecipitation sequencing (ChIP-seq) data from the Human Brain Transcriptome reveal that EZH2 expression in the anterior cingulate cortex is 3-fold higher in individuals with schizophrenia than in controls.⁷¹ In addition, studies have shown that cocaine exposure is closely associated with histone 3 lysine 9 (H3K9) dimethylation and that the lysine dimethyltransferase G9a induces EZH2 expression and structural and behavioral plasticity.^{72,73}

LINC01133 has been shown to interact with EZH2 and LSD1 scaffolds for promoter suppression of KLF2, P21, or E-cadherin.⁷⁴ In glioma patients, EZH2 overexpression is associated with increased glucose metabolism.⁷⁵ These findings prove that dysregulated expression of LINC01133 is associated with energy metabolism. However, the role of LINC01133 has not yet been elucidated in the context of HIV infection- and cocaine use-associated neurodegeneration. We investigated the effect of silencing LINC01133 expression and further studied the downstream effects on gene and miRNA expression. siRNA targeting LINC01133 resulted in downregulation of NDUFA9 gene expression but upregulation of hsa-miR-4726-5p expression. Overall, these results confirm that the interactions of the LINC01133-hsa-miR-4726-5p-NDUFA9 axis can be studied in the context of HANDs. The analyses allowed us to perform a robust comparative genomics and bioinformatics study to reveal a molecular signature of miRNAs, lncRNAs, and their mRNA/gene targets associated with HIV-1 TC in human primary astrocytes.

In summary, we identified four gene targets of two DE miRNAs and four lncRNAs involved in various biological processes using functional annotation with the KEGG database. The results of this integrative and multifaceted bioinformatics analysis form a comprehensive resource that provides novel insights into how significant lncRNA-miRNA-mRNA signature markers are regulated during HIV-1 infection with cocaine exposure via modulation of targeted metabolic pathways and pathways of neurodegeneration. However, further functional evaluation of the identified lncRNA, miRNA, and mRNA associations is needed to achieve a comprehensive mechanistic understanding of the roles of these molecules in HIV-1 Tat- and cocaine-mediated astrocyte dysfunction.

MATERIALS AND METHODS

Cell culture and reagents

Cocaine (purity >99%) was purchased from Sigma-Aldrich (CAS; St. Louis, MO, USA). Cell culture reagents were purchased from ScienCell (Carlsbad, CA, USA).

HIV-1 Tat proteins

HIV-1 Tat (catalog no. 2222) was obtained from the NIH AIDS Research and Reference Reagent Program. The recombinant Tat proteins were tested and revealed to be of >95% purity.

Human primary astrocytes

In this study, human primary astrocytes (isolated from the cerebral cortex) were obtained from ScienCell (CAT-1800). The cultured cells were maintained in basal astrocyte medium supplemented with a concentration of 1% astrocyte growth supplements (AGSs) and 10% fetal bovine serum (FBS) (ScienCell; Carlsbad, CA, USA).

Drug treatment *in vitro*

Cocaine was prepared in cell culture-grade distilled water to obtain working concentrations. To investigate the effects of HIV-1 Tat and cocaine on cultured cells, we divided the cells into four groups: (1) control cells exposed to medium alone, (2) cells treated with HIV-1 Tat (50 ng/mL), (3) cells exposed to cocaine (1 μ M), and (4) cells exposed to HIV-1 Tat (50 ng/mL) and cocaine (1 μ M) (TC) in combination for 24 h. The optimized doses and times used in the present studies were based on our published report.^{62,76}

Animals and housing

Adult male iTat mice (formerly known as GT-tg bigenic mice)⁷⁷ were bred from a colony started by progenitors generously donated by Dr. Johnny He. All mice (8–10 weeks of age) were maintained at the University of Florida's animal facilities and used in experiments according to protocols approved by the Institutional Animal Care and Use Committee of the University of Florida (Gainesville, FL, USA). The procedures for creating HIV-1 iTat mice and confirming the genotype for the inducible and brain-targeted HIV-1 Tat protein are described in detail elsewhere.^{77,78}

Drug treatment *in vivo*

Brain-targeted Tat was induced with doxycycline (Dox) treatment with or without cocaine exposure. To induce the expression of HIV-1 Tat [1–86], we administered Dox to iTat mice via intraperitoneal (i.p.) injection of a single daily dose of 100 mg/kg dissolved in 0.9% saline in a volume of 0.3 mL/30 g body weight for 14 days (iTat-Dox; n = 3). iTat mice treated with saline served as controls (n = 3), as indicated and characterized previously [41]. An additional set of mice received cocaine via subcutaneous (s.c.) administration at a dose of 10 mg/kg/day in 0.9% saline for 14 days (n = 3). A final set of iTat mice (n = 3) were treated with Dox (100 mg/kg/day, i.p.) followed by cocaine (10 mg/kg/day, s.c.) 2 min later.

Isolation of brain specimens for immunoblot analysis

After the 14-day treatment period, the mice were anesthetized with isoflurane (4%), euthanized, and subjected to transcardial perfusion with cold saline (0.9%), and tissues were harvested. The frontal lobe region of the brain was extracted from three euthanized mice for each treatment set, flash frozen in liquid nitrogen, and stored at -80°C for further analysis of gene and protein modifications.

RNA extraction

Total RNA was extracted from the primary astrocytes after 24 h of treatment using a Qiagen RNeasy Mini Kit (catalog no. 74104) (Germantown, MD, USA). The detailed procedures were carried out per manufacturer's instructions and a previously published paper.¹⁵ All experiments were repeated in triplicate to ensure the reproducibility of the data.

lncRNA-seq and DE analysis

RNA-seq library preparation was performed as per the manufacturer's instructions (Illumina, San Diego, CA, USA). The sequencing was performed on the Illumina HiSeq instrument (4000 or equivalent) according to the manufacturer's instructions. For lncRNA expression profiles, we applied the Limma-Voom R package to identify DE lncRNAs from given a matrix of featureCounts files. We investigated DE lncRNAs between the control and treatment groups using the "model.matrix," "lmFit," "eBays," and "topTable" functions.^{79–82} We also calculated the $\log_2\text{FC}$ values for each lncRNA by dividing the expression in the treated samples with the measured expression in the control counterparts. The statistical significance threshold was set at $p < 0.05$.

Small-RNA library preparation and HiSeq sequencing

RNA library preparation and sequencing were conducted at GENEWIZ (South Plainfield, NJ, USA). The detailed procedures for Small-RNA library preparation and HiSeq sequencing are discussed in a previously published paper.¹⁵

Small-RNA genomic analysis

The .fastq files for all samples were analyzed on Galaxy interface servers.⁸³ All reads were then further assessed through FastQC v0.72 for standard QC and trimmed⁸⁴ with Trim Galore version 0.6.3.⁸⁵ Low-quality reads and all reads < 18 nt in length were discarded by using Trim Galore. Reads 18–45 nt in length were then aligned to the *Homo sapiens* Hg38 reference genome downloaded from the Ensembl website (Homo_sapiens.GRCh38.89.chr.gtf.gz) with the sR_Bowtie tool (small-RNA short reads; Galaxy version 2.1.1) (one mismatch allowed).⁸⁶ The tool featureCounts used for miRNA counts measure from mapped .bam files with the help of a gene annotation file in .gtf format (from miRBase V22). For miRNA expression profiles, we applied the Limma-Voom R package to identify DE miRNAs using the "model.matrix," "lmFit," "eBays," and "topTable" functions.^{79–82} The statistical significance threshold was set at $p < 0.05$.

The miRDeep2⁸⁷ Mapper module mapped the .fastq files and performed the quantification of known miRNAs and prediction of po-

tential novel miRNAs.⁸⁸ The collapsed .fasta files were then used as input files in the web server sRNAtools.⁸⁹

miRNA extraction and quantitative real-time PCR assay

Astrocytes were seeded in 100-mm-diameter culture dishes at a density of 2×10^6 cells/dish. At the time of treatment, the astrocytes had reached approximately 65%–70% confluency. The total RNA extraction procedure using Qiagen miRNeasy Tissue/Cells Advanced Mini Kit (50) (catalog no. 217004; Qiagen, Germantown, MD, USA) was performed as per manufacturer's instructions. The total RNA was screened for purity according to a 260/280 ratio of ~ 2.0 . cDNA was synthesized and amplified using specific primers for hsa-miR-4726-5p (assay ID 463408_mat, catalog no. 4440885), hsa-miR-2355-5p (assay ID 241374_mat, catalog no. 4427975), and U6 snRNA (assay ID 001973, catalog no. 4427975) (Applied Biosystems, Foster City, CA, USA). For quantitative real-time PCR, U6 snRNA was used as an internal control. Initial denaturation was performed at 95°C for 2 min and was followed by 40 cycles of denaturation at 94°C for 15 s, annealing at 59°C for 1 min, and extension at 72°C for 15 s. The relative mRNA expression was quantified, and the $2^{-\Delta\Delta\text{CT}}$ method was used to calculate the FCs in the expression of the target miRNAs. All experiments were repeated in triplicate to ensure the reproducibility of the data.

lncRNA and mRNA analysis using real-time PCR

Astrocytes were seeded in 100-mm-diameter culture dishes at a density of 2×10^6 cells/dish. Total RNA extraction procedure using Qiagen RNeasy Tissue/Cells Mini Kit (50) (catalog no. 74104; Qiagen, Germantown, MD, USA) was performed as per the manufacturer's instructions. Total RNA was screened for purity according to a 260/280 ratio of ~ 2.0 . cDNA was synthesized and amplified using specific primers for NDUFA9 (assay ID Hs00245308_m1, catalog no. 4448892), LIPG (assay ID Hs00195812_m1, catalog no. 4331182), NOP14-AS1 (assay ID Hs03653612_m1, catalog no. 4331182), HHIP-AS1 (assay ID Hs04232235_m1, catalog no. 4426961), LINC01133 (assay ID Hs04274447_m1, catalog no. 4331182), H19 (assay ID Hs00399294_g1, catalog no. 4453320), and β -actin (Hs99999903_m1) (Applied Biosystems, Foster City, CA, USA). For quantitative real-time PCR, β -actin was used as an internal control. Initial denaturation was performed at 95°C for 2 min and was followed by 40 cycles of denaturation at 94°C for 15 s, annealing at 59°C for 1 min, and extension at 72°C for 15 s. The relative mRNA expression was quantified, and the $2^{-\Delta\Delta\text{CT}}$ method was used to calculate the FCs in the expression of the target mRNAs. All experiments were repeated in triplicate to ensure the reproducibility of the data.

Western blot analysis

An NDUFA9 rabbit polyclonal antibody (pAb) (A3196), LIPG rabbit pAb (A1891), KYNU rabbit pAb (A6643), and HKDC1 rabbit pAb (A16573) were purchased from ABclonal (Woburn, MA, USA) for expression analysis by western blotting. The detailed procedure of western blot experiment analysis was described in a previously published paper.¹⁵

Target gene prediction

miRNA target genes were identified using miRWalk 2.0.^{90,91} We used an approach in which the miRWalk 2.0 algorithm examined potential miRNA binding sites at the promoter, 5' UTR, and CDS of genes. We chose TargetScan, miRTarBase, and miRDB to validate the miRNA-target gene prediction scores. The miRNAs of the control and treated groups were compared, and the intersecting miRNAs were displayed using Venn diagrams (<http://bioinformatics.psb.ugent.be/webtools/Venn/>). The KEGG was employed for gene pathway annotation.⁹²⁻⁹⁴ A corrected $p < 0.05$ indicated statistical significance. Hierarchical categories were obtained based on the KEGG database.

siRNA knockdown

For primary astrocytes, the Lipofectamine RNAiMAX (μL):siRNA (pmol) ratio was 1:1, with a final total siRNA concentration of 30 pmol (six-well plate). Silencer Select Negative Control No. 1 (catalog no. 4390843) was used as a control. Silencer Select GAPDH Positive Control siRNA was used as a positive control (catalog no. 4390849). siLINC01133 was also used (assay ID s444575, catalog no. 4392420). The experiment was performed following the manufacturer's protocol. We utilized Opti-MEM I Reduced Serum Medium (catalog no. 31985062) and Lipofectamine RNAiMAX (catalog no. 13778100) Transfection Reagent for siRNA transfection. The siRNA oligonucleotides used are listed in Table S2. Forty-eight hours post-transfection, the medium for the primary astrocytes was changed to reduced-serum (2%) or serum-free medium without treatment (control) or containing HIV-1 Tat, cocaine, or TC, and the cells were harvested for RNA extraction at 72 h.

Systematic bioinformatics analysis to curate lists of lncRNAs and their targeted genes

To understand the interactions between lncRNAs and miRNAs, we utilized DIANA-LncBase v3, which is a reference repository with experimentally supported miRNA targets on noncoding transcripts.^{95,96} To decipher the interactions between lncRNAs and mRNAs, we utilized LncBook⁹⁷ and LncExpDB.⁹⁸ The interactions between various lncRNAs and other lncRNAs or mRNAs were analyzed using LncRRISearch, a web server for comprehensive prediction of human and mouse lncRNA-lncRNA and lncRNA-mRNA interactions. LncRRISearch uses RIBlast, which is a fast and accurate RNA-RNA interaction prediction tool. This tool can be used to investigate interactions of a particular lncRNA with target RNAs through a web interface. In addition, it integrates tissue-specific expression and subcellular localization data for lncRNAs with the web server.⁹⁹

Statistical analysis

Statistical analysis was performed using GraphPad Prism version 6. For comparisons of two groups, Student's two-tailed t test was performed. For comparisons of more than two groups, two-way ANOVA followed by Tukey's post hoc test was performed. All data are presented as the mean \pm standard error of the mean (SEM), and $p < 0.05$ was considered to indicate statistical significance.

DATA AVAILABILITY

The authors confirm that the data supporting the findings of this study are available within the article and/or its supplementary materials.

SUPPLEMENTAL INFORMATION

Supplemental information can be found online at <https://doi.org/10.1016/j.omtn.2022.07.001>.

ACKNOWLEDGMENTS

This work was supported by grants from the National Institute on Drug Abuse (NIDA) (R01 DA044872 to T.S.).

AUTHOR CONTRIBUTIONS

M.D. performed the experiment, acquired the data, analyzed the data, and drafted the manuscript. J.P.M. was involved in the HIV-iTat/cocaine mouse model studies; J.J.C. was involved in the bioinformatics data analysis; and G.P., M.A.K., and F.K. were involved in the data interpretation and revision of the manuscript. T.S. contributed to the study conception, study design, data interpretation, and drafting and revision of the manuscript. All authors read the manuscript and approved it for publication.

DECLARATION OF INTERESTS

The authors declare no competing interests.

REFERENCES

- Mohamed, A.A., Oduor, C., and Kinyanjui, D. (2020). HIV-associated neurocognitive disorders at Moi teaching and referral hospital, Eldoret, Kenya. *BMC Neuro* 20, 280.
- Esmaili, P., Boissier, N., and Valcour, V. (2015). HIV-Associated neurocognitive disorder (HAND) - family caregiver alliance. *Fam. Caregiv. Alliance*. <https://www.caregiver.org/resource/hiv-associated-neurocognitive-disorder-hand/>.
- Francisco, U. of C.S (2021). What Is Dementia? | Memory and Aging Center (Univ. Calif. San Fr. Weill Inst. Neurosci).
- Doherty, M.C., Garfein, R.S., Monterroso, E., Brown, D., and Vlahov, D. (2000). Correlates of HIV infection among young adult short-term injection drug users. *AIDS* 14, 717-726.
- Aksenov, M.Y., Aksenova, M.V., Nath, A., Ray, P.D., Mactutus, C.F., and Booze, R.M. (2006). Cocaine-mediated enhancement of Tat toxicity in rat hippocampal cell cultures: the role of oxidative stress and D1 dopamine receptor. *Neurotoxicology* 27, 217-228.
- Dahal, S., Chitti, S.V.P., Nair, M.P.N., and Saxena, S.K. (2015). Interactive effects of cocaine on HIV infection: implication in HIV-associated neurocognitive disorder and neuroAIDS. *Front. Microbiol.* 6, 931.
- Bantle, C.M., Hirst, W.D., Weihofen, A., and Shlevkov, E. (2021). Mitochondrial dysfunction in astrocytes: a role in Parkinson's disease? *Front. Cell Dev. Biol.* 8, 1587.
- Murphy-Royal, C., Johnston, A.D., Boyce, A.K.J., Diaz-Castro, B., Instititoris, A., Peringod, G., Zhang, O., Stout, R.F., Spray, D.C., Thompson, R.J., et al. (2020). Stress gates an astrocytic energy reservoir to impair synaptic plasticity. *Nat. Commun.* 11, 2014.
- Thompson, K.A., McArthur, J.C., and Wesselingh, S.L. (2001). Correlation between neurological progression and astrocyte apoptosis in HIV-associated dementia. *Ann. Neurol.* 49, 745-752.
- Dickens, A.M., Yoo, S.W., Chin, A.C., Xu, J., Johnson, T.P., Trout, A.L., Hauser, K.F., and Haughey, N.J. (2017). Chronic low-level expression of HIV-1 Tat promotes a neurodegenerative phenotype with aging. *Sci. Rep.* 7, 1-11.

11. Li, M., Xu, P., Xu, Y., Teng, H., Tian, W., Du, Q., and Zhao, M. (2017). Dynamic expression changes in the transcriptome of the prefrontal cortex after repeated exposure to cocaine in mice. *Front. Pharmacol.* 8, 142.
12. Xu, H., Brown, A.N., Waddell, N.J., Liu, X., Kaplan, G.J., Chitaman, J.M., Stockman, V., Hedinger, R.L., Adams, R., Abreu, K., et al. (2020). Role of long noncoding RNA Gas5 in cocaine action. *Biol. Psychiatr.* 88, 758–766.
13. Qu, D., Sun, W.W., Li, L., Ma, L., Sun, L., Jin, X., Li, T., Hou, W., and Wang, J.H. (2019). Long noncoding RNA MALAT1 releases epigenetic silencing of HIV-1 replication by displacing the polycomb repressive complex 2 from binding to the LTR promoter. *Nucleic Acids Res.* 47, 3013–3027.
14. Ray, R.M., and Morris, K.V. (2020). Long non-coding RNAs mechanisms of action in HIV-1 modulation and the identification of novel therapeutic targets. *Noncoding RNA* 6, 12.
15. Doke, M., Kashanchi, F., Khan, M.A., and Samikkannu, T. (2021). HIV-1 Tat and cocaine impact astrocytic energy reservoir influence on miRNA epigenetic regulation. *Genomics* 113, 3461–3475.
16. Wang, L., Cho, K.B., Li, Y., Tao, G., Xie, Z., and Guo, B. (2019). Long noncoding RNA (lncRNA)-mediated competing endogenous RNA networks provide novel potential biomarkers and therapeutic targets for colorectal cancer. *Int. J. Mol. Sci.* 20, E5758.
17. Chuang, J.C., and Jones, P.A. (2007). Epigenetics and microRNAs. *Pediatr. Res.* 61, 24–29.
18. Orom, U.A., Derrien, T., Beringer, M., Gumireddy, K., Gardini, A., Bussotti, G., Lai, F., Zytnicki, M., Notredame, C., Huang, Q., et al. (2010). Long noncoding RNAs with enhancer-like function in human cells. *Cell* 143, 46–58.
19. Wang, K.C., and Chang, H.Y. (2011). Molecular mechanisms of long noncoding RNAs. *Mol. Cell* 43, 904–914.
20. Kyzar, E.J., Bohnsack, J.P., and Pandey, S.C. (2022). Current and future perspectives of noncoding RNAs in brain function and neuropsychiatric disease. *Biol. Psychiatry* 91, 183–193.
21. Statello, L., Guo, C.J., Chen, L.L., and Huarte, M. (2021). Gene regulation by long non-coding RNAs and its biological functions. *Nat. Rev. Mol. Cell Biol.* 22, 96–118.
22. López-Urrutia, E., Bustamante Montes, L.P., Ladrón de Guevara Cervantes, D., Pérez-Plasencia, C., and Campos-Parra, A.D. (2019). Crosstalk Between Long Non-coding RNAs, Micro-RNAs and mRNAs: Deciphering Molecular Mechanisms of Master Regulators in Cancer. *Front. Oncol.* 9, 669.
23. Herrera-Solorio, A.M., Armas-López, L., Arrieta, O., Zúñiga, J., Piña-Sánchez, P., and Ávila-Moreno, F. (2017). Histone code and long non-coding RNAs (lncRNAs) aberrations in lung cancer: implications in the therapy response. *Clin. Epigenet.* 9, 98.
24. Wilusz, J.E., Sunwoo, H., and Spector, D.L. Long noncoding RNAs: functional surprises from the RNA world.
25. Mercer, T.R., Dinger, M.E., and Mattick, J.S. (2009). Long non-coding RNAs: insights into functions. *Nat. Rev. Genet.* 10, 155–159.
26. Dhanoa, J.K., Sethi, R.S., Verma, R., Arora, S., and Mukhopadhyay, C.S. (2018). Long non-coding RNA: its evolutionary relics and biological implications in mammals: a review. *J. Anim. Sci. Technol.* 60, 25. <https://doi.org/10.1186/s40781-018-0183-7>.
27. Shen, L., Wu, C., Zhang, J., Xu, H., Liu, X., Wu, X., Wang, T., and Mao, L. (2020). Roles and potential applications of lncRNAs in HIV infection. *Int. J. Infect. Dis.* 92, 97–104.
28. Zhou, Z., Enoch, M.A., and Goldman, D. (2014). Gene expression in the addicted brain. In *International Review of Neurobiology* (NIH Public Access), pp. 251–273.
29. Belgard, T.G., Marques, A.C., Oliver, P.L., Abaan, H.O., Sirey, T.M., Hoerder-Suabedissen, A., García-Moreno, F., Molnár, Z., Margulies, E.H., and Ponting, C.P. (2011). A transcriptomic atlas of mouse neocortical layers. *Neuron* 71, 605–616.
30. Mercer, T.R., Dinger, M.E., Sunkin, S.M., Mehler, M.F., and Mattick, J.S. (2008). Specific expression of long noncoding RNAs in the mouse brain. *Proc. Natl. Acad. Sci. USA* 105, 716–721.
31. Gruner, H., Cortés-López, M., Cooper, D.A., Bauer, M., and Miura, P. (2016). CircRNA accumulation in the aging mouse brain. *Sci. Rep.* 6, 38907.
32. Sang, Q., Liu, X., Wang, L., Qi, L., Sun, W., Wang, W., Sun, Y., and Zhang, H. (2018). CircSNCA downregulation by pramipexole treatment mediates cell apoptosis and autophagy in Parkinson's disease by targeting miR-7. *Aging (Albany NY)* 10, 1281–1293.
33. Chung, D.W., Rudnicki, D.D., Yu, L., and Margolis, R.L. (2011). A natural antisense transcript at the Huntington's disease repeat locus regulates HTT expression. *Hum. Mol. Genet.* 20, 3467–3477.
34. Smillie, C.L., Sirey, T., and Ponting, C.P. (2018). Complexities of post-transcriptional regulation and the modeling of ceRNA crosstalk. *Crit. Rev. Biochem. Mol. Biol.* 53, 231–245.
35. Salmena, L., Poliseno, L., Tay, Y., Kats, L., and Pandolfi, P.P. (2011). A ceRNA hypothesis: the Rosetta Stone of a hidden RNA language? *Cell* 146, 353–358.
36. Shi, X., Sun, M., Liu, H., Yao, Y., and Song, Y. (2013). Long non-coding RNAs: a new frontier in the study of human diseases. *Cancer Lett.* 339, 159–166.
37. Balas, M.M., and Johnson, A.M. (2018). Exploring the mechanisms behind long non-coding RNAs and cancer. *Noncoding RNA Res.* 3, 108–117.
38. Dhanoa, J.K., Sethi, R.S., Verma, R., Arora, J.S., and Mukhopadhyay, C.S. (2018). Long non-coding RNA: its evolutionary relics and biological implications in mammals: a review. *J. Anim. Sci. Technol.* 60, 25.
39. Fernandes, J.C.R., Acuña, S.M., Aoki, J.I., Floeter-Winter, L.M., and Muxel, S.M. (2019). Long non-coding RNAs in the regulation of gene expression: physiology and disease. *Noncoding RNA* 5, 17.
40. Bartel, D.P. (2004). MicroRNAs: genomics, biogenesis, mechanism, and function. *Cell* 116, 281–297.
41. Guo, L., Zhao, Y., Yang, S., Zhang, H., and Chen, F. (2014). An integrated analysis of miRNA, lncRNA, and mRNA expression profiles. *Biomed Res. Int.* 2014, 345605.
42. Ray, R.M., and Morris, K.V. (2020). Long non-coding RNAs mechanisms of action in HIV-1 modulation and the identification of novel therapeutic targets. *Noncoding RNA* 6, 12.
43. Poelmans, G., Pauls, D.L., Buitelaar, J.K., and Franke, B. (2011). Integrated genome-wide association study findings: identification of a neurodevelopmental network for attention deficit hyperactivity disorder. *Am. J. Psychiatr.* 168, 365–377.
44. Irwin, D.M., and Tan, H. (2008). Molecular evolution of the vertebrate hexokinase gene family: Identification of a conserved fifth vertebrate hexokinase gene. *Comp. Biochem. Physiol. Part D Genomics Proteomics* 3, 96–107.
45. Hayes, M.G., Urbanek, M., Hivert, M.F., Armstrong, L.L., Morrison, J., Guo, C., Lowe, L.P., Scheftner, D.A., Pluzhnikov, A., Levine, D.M., et al. (2013). Identification of HKDC1 and BACE2 as genes influencing glycemic traits during pregnancy through genome-wide association studies. *Diabetes* 62, 3282–3291.
46. Fuhr, L., El-Athman, R., Scrima, R., Cela, O., Carbone, A., Knoop, H., Li, Y., Hoffmann, K., Laukkanen, M.O., Corcione, F., et al. (2018). The Circadian Clock Regulates Metabolic Phenotype Rewiring Via HKDC1 and Modulates Tumor Progression and Drug Response in Colorectal Cancer. *EBioMedicine* 33, 105–121.
47. Fuhr, L., El-Athman, R., Scrima, R., Cela, O., Carbone, A., Knoop, H., Li, Y., Hoffmann, K., Laukkanen, M.O., Corcione, F., et al. (2018). The Circadian Clock Regulates Metabolic Phenotype Rewiring Via HKDC1 and Modulates Tumor Progression and Drug Response in Colorectal Cancer. *EBioMedicine* 33, 105–121.
48. Sivalingam, K., Cirino, T.J., McLaughlin, J.P., and Samikkannu, T. (2020). HIV-Tat and Cocaine Impact Brain Energy Metabolism: Redox Modification and Mitochondrial Biogenesis Influence NRF Transcription-Mediated Neurodegeneration. *Mol. Neurobiol.* 58, 490–504.
49. Samikkannu, T., Atluri, V.S.R., and Nair, M.P.N. (2016). HIV and cocaine impact glial metabolism: Energy sensor AMP-activated protein kinase role in mitochondrial biogenesis and epigenetic remodeling. *Sci. Rep.* 6, 31784.
50. Murakami, K., Kanno, H., Tancabelic, J., and Fujii, H. (2002). Gene expression and biological significance of hexokinase in erythroid cells. *Acta Haematol.* 108, 204–209.

51. Keegan, M.R., Chittiprol, S., Letendre, S.L., Winston, A., Fuchs, D., Boasso, A., Iudicello, J., and Ellis, R.J. (2016). Tryptophan metabolism and its relationship with depression and cognitive impairment among HIV-infected individuals. *Int. J. Tryptophan Res.* 9, 79–88.
52. Samikkannu, T., Saiyed, Z.M., Rao, K.V.K., Babu, D.K., Rodriguez, J.W., Papuashvili, M.N., and Nair, M.P.N. (2009). Differential regulation of Lndoleamine-2, 3-dioxygenase (Ido) by HIV type 1 clade B and C tat protein. *AIDS Res. Hum. Retroviruses* 25, 329–335.
53. Valle, M., Price, R.W., Nilsson, A., Heyes, M., and Verotta, D. (2004). CSF quinolinic acid levels are determined by local HIV infection: cross-sectional analysis and modeling of dynamics following antiretroviral therapy. *Brain* 127, 1047–1060.
54. Heyes, M.P., Ellis, R.J., Ryan, L., Childers, M.E., Grant, I., Wolfson, T., Archibald, S., Jernigan, T.L.; HNRC Group HIV Neurobehavioral Research Center, and McCutchan, J.A., et al. (2001). Elevated cerebrospinal fluid quinolinic acid levels are associated with region-specific cerebral volume loss in HIV infection. *Brain* 124, 1033–1042.
55. Liu, H., Ding, L., Zhang, H., Mellor, D., Wu, H., Zhao, D., Wu, C., Lin, Z., Yuan, J., and Peng, D. (2018). The metabolic factor kynurenic acid of kynurenine pathway predicts major depressive disorder. *Front. Psychiatr.* 9, 552.
56. Fonseca, F., Mestre-Pintó, J.I., Gómez-Gómez, À., Martínez-Sanvisens, D., Rodríguez-Minguela, R., Papaseit, E., Pérez-Mañá, C., Langohr, K., Valverde, O., Pozo, Ó.J., et al. (2020). The tryptophan system in cocaine-induced depression. *J. Clin. Med.* 9, E4103.
57. Sharma, L.K., Lu, J., and Bai, Y. (2009). Mitochondrial respiratory complex I: structure, function and implication in human diseases. *Curr. Med. Chem.* 16, 1266–1277.
58. Gasparre, G., Porcelli, A.M., Lenaz, G., and Romeo, G. (2013). Relevance of mitochondrial genetics and metabolism in cancer development. *Cold Spring Harb. Perspect. Biol.* 5, a011411.
59. Hámor, P.U., Edelmann, M.J., Gobin, C., and Schwendt, M. (2020). Long-term changes in the central amygdala proteome in rats with a history of chronic cocaine self-administration. *Neuroscience* 443, 93–109.
60. Yu, J.E., Han, S.Y., Wolfson, B., and Zhou, Q. (2018). The role of endothelial lipase in lipid metabolism, inflammation and cancer. *Histol. Histopathol.* 33, 1–10.
61. Yu, J.E., Han, S.Y., Wolfson, B., and Zhou, Q. (2018). The role of endothelial lipase in lipid metabolism, inflammation, and cancer. *Histol. Histopathol.* 33, 1–10.
62. Doke, M., Jeganathan, V., McLaughlin, J.P., and Samikkannu, T. (2021). HIV-1 Tat and cocaine impact mitochondrial epigenetics: effects on DNA methylation. *Epigenetics* 16, 980–999.
63. Fan, Y., Xia, X., Zhu, Y., Diao, W., Zhu, X., Gao, Z., and Chen, X. (2018). Circular RNA Expression Profile in Laryngeal Squamous Cell Carcinoma Revealed by Microarray. *Cell. Physiol. Biochem.* 50, 342–352.
64. Hyun-jung, R. (2017). miR4324 as a Biomarker for Parkinson's Disease and Diagnostic Kit Using Thereof.
65. Li, Z., Xu, D., Chen, X., Li, S., Chan, M.T.V., and Wu, W.K.K. (2020). LINC01133: an emerging tumor-associated long non-coding RNA in tumor and osteosarcoma. *Environ. Sci. Pollut. Res. Int.* 27, 32467–32473.
66. Zhang, J., Zhu, N., and Chen, X. (2015). A novel long noncoding RNA LINC01133 is upregulated in lung squamous cell cancer and predicts survival. *Tumour Biol.* 36, 7465–7471.
67. Yang, X.Z., He, Q.J., Cheng, T.T., Chi, J., Lei, Z.Y., Tang, Z., Liao, Q.X., Zhang, H., Zeng, L.S., and Cui, S.Z. (2018). Predictive value of LINC01133 for unfavorable prognosis was impacted by alcohol in esophageal squamous cell carcinoma. *Cell. Physiol. Biochem.* 48, 251–262.
68. Li, Z., Xu, D., Chen, X., Li, S., Chan, M.T.V., and Wu, W.K.K. (2020). LINC01133: an emerging tumor-associated long non-coding RNA in tumor and osteosarcoma. *Environ. Sci. Pollut. Res. Int.* 27, 32467–32473.
69. Briata, P., and Gherzi, R. (2020). Long non-coding RNA-ribonucleoprotein networks in the post-transcriptional control of gene expression. *Noncoding. RNA* 6, E40.
70. Zhang, H.S., Liu, Y., Wu, T.C., Du, G.Y., and Zhang, F.J. (2015). EZH2 phosphorylation regulates Tat-induced HIV-1 transactivation via ROS/Akt signaling pathway. *FEBS Lett.* 589, 4106–4111.
71. Billingsley, K.J., Manca, M., Gianfrancesco, O., Collier, D.A., Sharp, H., Bubb, V.J., and Quinn, J.P. (2018). Regulatory characterisation of the schizophrenia-associated CACNA1C proximal promoter and the potential role for the transcription factor EZH2 in schizophrenia aetiology. *Schizophr. Res.* 199, 168–175.
72. Maze, I., Covington, H.E., 3rd, Dietz, D.M., Laplant, Q., Renthal, W., Russo, S.J., Mechanic, M., Mouzon, E., Neve, R.L., Haggarty, S.J., et al. (2010). Essential role of the histone methyltransferase G9a in cocaine-induced plasticity. *Science* 327, 213–216.
73. Zheng, Y., He, L., Wan, Y., and Song, J. (2013). H3K9me-enhanced DNA hypermethylation of the p16INK4a gene: an epigenetic signature for spontaneous transformation of rat mesenchymal stem cells. *Stem Cells Dev.* 22, 256–267.
74. Dempsey, J.L., and Cui, J.Y. (2017). Long non-coding RNAs: a novel paradigm for toxicology. *Toxicol. Sci.* 155, 3–21.
75. Wang, Y., Wang, M., Wei, W., Han, D., Chen, X., Hu, Q., Yu, T., Liu, N., You, Y., Zhang, J., et al. (2016). Disruption of the EZH2/miRNA/ β -catenin signaling suppresses aerobic glycolysis in glioma. *Oncotarget* 7, 49450–49458.
76. Sivalingam, K., and Samikkannu, T. (2020). Neuroprotective effect of piracetam against cocaine-induced neuro epigenetic modification of DNA methylation in astrocytes. *Brain Sci.* 10, 611.
77. Kim, B.O., Liu, Y., Ruan, Y., Xu, Z.C., Schantz, L., and He, J.J. (2003). Neuropathologies in transgenic mice expressing human immunodeficiency virus type 1 Tat protein under the regulation of the astrocyte-specific glial fibrillary acidic protein promoter and doxycycline. *Am. J. Pathol.* 162, 1693–1707.
78. Paris, J.J., Singh, H.D., Ganno, M.L., Jackson, P., and McLaughlin, J.P. (2014). Anxiety-like behavior of mice produced by conditional central expression of the HIV-1 regulatory protein. *Psychopharmacology* 231, 2349–2360.
79. Smyth, G.K. (2004). Linear models and empirical bayes methods for assessing differential expression in microarray experiments. *Stat. Appl. Genet. Mol. Biol.* 3.
80. Phipson, B., Lee, S., Majewski, I.J., Alexander, W.S., and Smyth, G.K. (2016). Robust hyperparameter estimation protects against hypervariable genes and improves power to detect differential expression. *Ann. Appl. Stat.* 10, 946–963.
81. Ritchie, M.E., Phipson, B., Wu, D., Hu, Y., Law, C.W., Shi, W., and Smyth, G.K. (2015). Limma powers differential expression analyses for RNA-sequencing and microarray studies. *Nucleic Acids Res.* 43, e47.
82. Law, C.W., Chen, Y., Shi, W., and Smyth, G.K. (2014). Voom: precision weights unlock linear model analysis tools for RNA-seq read counts. *Genome Biol.* 15, R29.
83. Afgan, E., Baker, D., Batut, B., Van Den Beek, M., Bouvier, D., Cech, M., Chilton, J., Clements, D., Coraor, N., Grünig, B.A., et al. (2018). The Galaxy platform for accessible, reproducible and collaborative biomedical analyses: 2018 update. *Nucleic Acids Res.* 46, W537–W544.
84. Andrews, S. Babraham bioinformatics - FastQC A quality control tool for high throughput sequence data. *Soil* 5, 47–81.
85. Krueger, F. (2017). Babraham Bioinformatics - Trim Galore! Version 0.4.4. http://www.bioinformatics.babraham.ac.uk/projects/trim_galore/.
86. Langmead, B., Trapnell, C., Pop, M., and Salzberg, S.L. (2009). Ultrafast and memory-efficient alignment of short DNA sequences to the human genome. *Genome Biol.* 10, R25.
87. Friedländer, M.R., MacKowiak, S.D., Li, N., Chen, W., and Rajewsky, N. (2012). MiRDeep2 accurately identifies known and hundreds of novel microRNA genes in seven animal clades. *Nucleic Acids Res.* 40, 37–52.
88. Kozomara, A., and Griffiths-Jones, S. (2014). MiRBase: annotating high confidence microRNAs using deep sequencing data. *Nucleic Acids Res.* 42, D68–D73.
89. Liu, Q., Ding, C., Lang, X., Guo, G., Chen, J., and Su, X. (2019). Small noncoding RNA discovery and profiling with sRNATools based on high-throughput sequencing. *Brief. Bioinform.*
90. Dweep, H., Sticht, C., Pandey, P., and Gretz, N. (2011). MiRWalk - database: prediction of possible miRNA binding sites by “walking” the genes of three genomes. *J. Biomed. Inform.* 44, 839–847.
91. Dweep, H., and Gretz, N. (2015). MiRWalk2.0: a comprehensive atlas of microRNA-target interactions. *Nat. Methods* 12, 697.

92. Kanehisa, M. (2019). Toward understanding the origin and evolution of cellular organisms. *Protein Sci.* *28*, 1947–1951.
93. Kanehisa, M., Furumichi, M., Sato, Y., Ishiguro-Watanabe, M., and Tanabe, M. (2021). KEGG: integrating viruses and cellular organisms. *Nucleic Acids Res.* *49*, D545–D551.
94. Kanehisa, M., and Goto, S. (2000). KEGG: kyoto encyclopedia of genes and genomes. *Nucleic Acids Res.* *28*, 27–30.
95. Karagkouni, D., Paraskevopoulou, M.D., Tastsoglou, S., Skoufos, G., Karavangeli, A., Pierros, V., Zacharopoulou, E., and Hatzigeorgiou, A.G. (2020). DIANA-LncBase v3: indexing experimentally supported miRNA targets on non-coding transcripts. *Nucleic Acids Res.* *48*, D101–D110.
96. Paraskevopoulou, M.D., Karagkouni, D., Vlachos, I.S., Tastsoglou, S., and Hatzigeorgiou, A.G. (2018). microCLIP super learning framework uncovers functional transcriptome-wide miRNA interactions. *Nat. Commun.* *9*(1), 1–16.
97. Ma, L., Cao, J., Liu, L., Du, Q., Li, Z., Zou, D., Bajic, V.B., and Zhang, Z. (2019). Lncbook: a curated knowledgebase of human long non-coding rnas. *Nucleic Acids Res.* *47*, 2699.
98. Li, Z., Liu, L., Jiang, S., Li, Q., Feng, C., Du, Q., Zou, D., Xiao, J., Zhang, Z., and Ma, L. (2021). LncExpDB: an expression database of human long non-coding RNAs. *Nucleic Acids Res.* *49*, D962–D968.
99. Fukunaga, T., Iwakiri, J., Ono, Y., and Hamada, M. (2019). Lncrisearch: a web server for lncRNA-RNA interaction prediction integrated with tissue-specific expression and subcellular localization data. *Front. Genet.* *10*, 462.